



Quantitative assessment of diabetic amyotrophy using magnetic resonance neurography—a case-control analysis

Rocco Hlis¹ · Feng Poh^{1,2} · Meredith Bryarly¹ · Yin Xi¹ · Avneesh Chhabra¹

Received: 30 November 2018 / Revised: 19 February 2019 / Accepted: 14 March 2019 / Published online: 12 April 2019
© European Society of Radiology 2019

Abstract

Objectives To quantitatively characterize diabetic amyotrophy (DA), or diabetic lumbosacral radiculoplexopathy, and compare with controls using magnetic resonance neurography (MRN).

Methods Forty controls and 23 DA cases were analyzed qualitatively and quantitatively. Cross-sectional areas (CSAs) of bilateral L3 through S2 lumbosacral nerve roots, femoral nerves, and sciatic nerves (proximal and distal measurements) were measured. A linear model was used to assess the nerve location and case/control effect on angle-corrected CSAs. Intra- and inter-reader analysis was performed using intraclass correlation (ICC).

Results In DA cases, abnormalities of the lumbosacral nerve roots, sciatic, femoral, and obturator nerves were seen in 21/23, 16/23, 21/23, and 9/23, respectively. Denervation abnormalities of multiple abdominopelvic muscles were seen. Quantitatively, the CSA of all measured LS plexus nerve roots and bilateral femoral nerves were significantly larger in DA cases vs. controls by 45% (95% CI, (30%, 49%); $p < 0.001$). The ICC was moderate for inter-rater analysis = 0.547 (95% CI, 0.456–0.626) and excellent for intra-rater analysis = 0.90 (95% CI, 0.89–92).

Conclusions Multifocal neuromuscular lesions related to diabetic amyotrophy were qualitatively and quantitatively detected on MRN. Qualitative abnormalities distinguished cases from controls, and nerve CSAs of cases were significantly larger than those of controls. Therefore, MRN may be employed as a non-invasive diagnostic tool for the evaluation of diabetic amyotrophy.

Key Points

- *Qualitative abnormalities of lumbosacral nerve roots, their peripheral branches, and muscles are seen in DA.*
- *The lumbosacral nerve roots and their peripheral branches in diabetic amyotrophy cases are significantly larger in cross-sectional area than non-diabetic subjects by 45% (95 CI, 30%, 49%; $p < 0.001$).*
- *The ICC was moderate for inter-rater analysis = 0.547 (95% CI, 0.456–0.626) and excellent for intra-rater analysis = 0.90 (95% CI, 0.89–92).*

Keywords Magnetic resonance imaging · Diabetic amyotrophy · Lumbosacral plexus · Diabetic neuropathies

Abbreviations

CSA Cross-sectional area
DA Diabetes amyotrophy
DRG Dorsal nerve root ganglion
EMG Electromyography

ICC Intraclass correlation coefficient
LS Lumbosacral
MRI Magnetic resonance imaging
MRN Magnetic resonance neurography
NCS Nerve conduction studies

✉ Avneesh Chhabra
avneesh.chhabra@utsouthwestern.edu

¹ UT Southwestern Medical Center, 5323 Harry Hines Blvd, Dallas, TX 75390-9178, USA

² Medi-Rad Associates Ltd, Radiologic Clinic, Mt Elizabeth Hospital, 3 Mount Elizabeth, Singapore 228510, Singapore

Introduction

Diabetes mellitus is an important condition with an estimated prevalence of 12.2% in adults over 18 years old [1]. It is the seventh leading cause of death as the individuals living with diabetes carry an excessive risk of death of 15% [2]. Thus, not surprisingly, diabetes places a significant burden on US

healthcare with a total estimated healthcare cost of \$245 billion in 2012 [3].

Diabetic neuropathy is believed to be related to damage to the vascular supply of the nerves (*vasa nervosa*) and/or deposition of advanced glycosylation products in the intraneural space [4]. Diabetic amyotrophy (DA), or diabetic lumbosacral radiculoplexopathy, refers to a proximal diabetic neuropathy of the lumbosacral (LS) plexus that affects the hips, thighs, buttocks, or lower legs. The symptoms and clinical findings frequently mimic radiculopathy, plexopathy, or invasive or inflammatory neuropathies. It has been reported that there is no good correlation of development of DA with HbA1c levels and even patients with minimally elevated blood levels can develop a severe DA [5].

Conventional MRI (e.g., pelvic/hip/lumbar spine) displays excellent detail of the soft tissues thereby providing information regarding muscle denervation; however, it does not show detailed nerve architecture and signal alterations that are abnormal in DA [6–8].

Nerve conduction studies/electromyography (NCS/EMG) may aid in the diagnosis of DA. However, these studies may be limited by the inability to localize and differentiate true lesions from a common mimicker, or from an entirely different radiculopathic etiology. There may also be practical drawbacks which include invasiveness and discomfort for patients [9]. Electrophysiology results are useful for functional assessment; however, limitations may arise for deeply located nerves, especially in obese patients, and results may vary with alterations of temperature and pH [10–12]. While electrophysiology may help in describing chronicity, localization, and character (i.e., demyelinating vs. axonal) of lesions, the diagnosis of focal entrapment versus diffuse abnormality and organic lesions is best accomplished using magnetic resonance neurography (MRN) imaging in conjunction with EMG/NCS [13–16].

The utility of MRN for characterization of diabetic nerve lesions in the lower extremity and plexus has been previously reported [17–19]. However, there has been no previous systematic scientific investigation of the use of MRI or MRN in the evaluation of DA. The authors sought to systematically characterize neuromuscular lesions on MRN in this case-control study. Our hypothesis was that DA shows a wide spectrum of neuromuscular abnormalities on MRN, and quantitative nerve caliber alterations can distinguish cases from the controls.

Materials and methods

Standard protocol approvals, registrations, and patient consents

This is a retrospective cross-sectional evaluation following the Health Insurance Portability and Accountability Act and

Institutional Review Board guidelines. Institutional Review Board approval was obtained, and informed consent was waived.

DA and controls

DA (case) group: A search of the university hospital and affiliated county hospital electronic medical records was performed yielding 23 DA from 7/15/2013 through 5/18/2018 who completed MRN LS plexus studies. Exclusion criteria included no established clinical diagnosis of DA, no known diagnosis of diabetes or prediabetes, and poor image quality.

Control group: A search of the hospital electronic medical records was performed yielding 40 consecutive patients from 10/31/2014 through 4/18/2018 with normal MRN findings of the LS plexus and regional muscles. The indications for MRN were groin pain or testicular pain (suspected genitofemoral or pudendal neuralgia). Exclusion criteria included a diagnosis of diabetes or prediabetes, presence of surgical hardware, suspected radiculopathy, lumbosacral plexus findings of neuropathy, abnormal femoral, obturator, or sciatic nerve findings, muscle denervation or myopathy findings, and poor image quality. Other confounding diagnoses, such as monoclonal gammopathy, vitamin B deficiency, and radiation exposure to the lumbosacral region were excluded. Basic demographic data gathered from the electronic records included age, sex, BMI, and the magnetic field strength.

An electronic chart review was completed from 4/9/2018 through 4/12/2018 to record the following characteristics: age; sex; history of diabetes (in years); HbA1C closest to the time of MRN LS plexus; the highest recorded HbA1C; the number of prior indeterminate or non-contributory MRIs of the lumbar spine, pelvis, and lower extremity; presenting motor, sensory, and pain symptoms; laterality of symptoms or clinical findings; electrophysiology procedure date and relevant findings; and magnetic field strength of the performed MRNs.

The MRN reports were assessed for abnormal nerve findings (increased signal or enlargement), muscle findings (edema, atrophy, and/or fatty infiltration), and moderate to severe degenerative disc and joint disease of the LS spine, as the resultant radiculopathy findings can mimic DA. The normal nerve roots gradually decrease in signal and size distal to the dorsal nerve root ganglion (DRG) and are symmetrical in both signal intensity and caliber as compared with side to side. The lack of normal fading of signal or increased signal or size (focal &/or diffuse) as well as asymmetry was used to detect the lesions in the lumbosacral nerves. The nerve findings were recorded with respect to the lumbosacral plexus nerve roots and to the femoral, obturator, and sciatic nerves. The muscle evaluated included the para-spinal, iliacus, psoas, three gluteals, quadratus femoris, seven adductors (adductor brevis, adductor longus, adductor magnus, adductor minimus, pectineus, gracilis, obturator externus), and the proximal

quadriceps. The abnormalities, originally detected by fellowship-trained musculoskeletal radiologists as standard of care, were reviewed from the MRN reports by a medical student, and these were further confirmed on re-review by two fellowship-trained musculoskeletal radiologists.

The electrophysiology studies were assessed by a fellowship-trained neuromuscular neurologist who was blinded to the final diagnosis of each case, and to the intent and contents of this study. Before reviewing each study, the neuromuscular specialist was provided the clinical history, examination findings, and relevant laboratory findings of each patient. The neurologist's impression along with up to five differential diagnoses in order of descending likelihood was recorded.

MR image acquisition

The MRN of LS plexuses were performed on high-field scanners (1.5-T and 3-T magnets); all were non-contrast examinations with the exception of 6 control patients and 5 DA patients. Only non-contrast images were evaluated for uniformity purposes. The protocol for a 3-T scanner is outlined in Table 1. A combination of large torso coil and posterior spine coil elements was used for imaging. 3-dimensional 1.5-mm isotropic images were used for LS plexus and peripheral nerve evaluation for all scans. Axial diffusion tensor images were used for qualitative neuromuscular signal alterations along with axial fat-suppressed T2-weighted images during the initial readings of these studies as standard of care. Axial fat-suppressed T2-weighted and T1-weighted images were also used for muscle signal and atrophy evaluation. The image quality of the examination was assessed by a musculoskeletal radiologist as per the following categories: motion (absent:0, mild:1, moderate:2, severe:3, non-diagnostic:4), fat suppression (poor:1, suboptimal:2, good:3, excellent:4), and overall image quality (poor:1, suboptimal:2, satisfactory:3, good:4, excellent:5).

Data collection

For both control and lesion groups, freehand ROI were drawn by two independent readers (a medical student, R1; and a radiologist, R2) for quantitative analysis from 4/16/2018

through 5/14/2018. The measurements encompassed bilateral L3, L4, L5, S1, S2, femoral (at L5 nerve root level in the iliopsoas triangle), and sciatic nerves (at ischial spine, proximal level and tuberosity, distal level), and were recorded from the axial fat-suppressed T2-weighted sequence yielding ROI cross-sectional areas (CSA) as seen in Fig. 1. The perineural fat was carefully excluded. The readers completed a training session with 5 cases together and performed independent measurements afterward, blinded to the final clinical diagnosis. For inter-observer performance, reader R2 measured all nerves in one-third of the data set, randomly chosen from the full data set. Reader R1 then re-measured all nerves of interest using the same methodology, approximately 6 months after the initial measurements were obtained.

Nerve trajectory angle correction factor

The centroids of two corresponding nerve CSAs in consecutive axial slices were identified for all patients. The distance between centroids and the distance between slices was used to calculate the angle between nerve trajectory and axial slice plane using the following equation: $\alpha = \arctangent\left(\frac{\text{distance between centroids}}{\text{distance between slices}}\right)$. The cosine (α) was multiplied by each CSA before analysis to account for increased CSAs secondary to deviation from the axis perpendicular to the acquired axial slice. A detailed derivation of the correction is depicted in Fig. 2.

Statistical analysis

Descriptive statistics were performed for demographic variables, and for qualitative findings from the MRN reads. The association between laterality of nerve findings and presenting symptoms was tested by a χ^2 test and quantified by the Φ coefficient which was calculated as dividing the χ^2 statistic by the sample size and taking the square root of the result. A random-subject random-rater two-way model with absolute agreement intraclass correlation coefficient (ICC) was performed between reader 1 and reader 2 for inter-rater analysis. Reader 1 re-measured all nerves approximately 6 months after initial measurements. A similar intraclass correlation

Table 1 3-T magnetic resonance neurography protocol

Pulse sequence	2-D/3-D	TR (ms)	TE (ms)	Slice thickness (mm)	Coverage
Axial T1W	2-D	700	8	4	T12 to L1 to lesser trochanters
Axial T2 SPAIR	2-D	4800	65	4	T12 to L1 to lesser trochanters
Coronal IR TSE	3-D	2000	78	1.5 isotropic	T12 to L1 to lesser trochanters
Sagittal T2 TSE	3-D	2000	120	0.9 isotropic	T12 to L1 to sacrum
Axial DTI	2-D	6000	65	4	T12 to L1 to lesser trochanters

2-D/3-D 2-dimensional/3-dimensional, TR repetition time, TE echo time, SPAIR spectral adiabatic inversion recovery, IR inversion recovery, TSE turbo spin echo

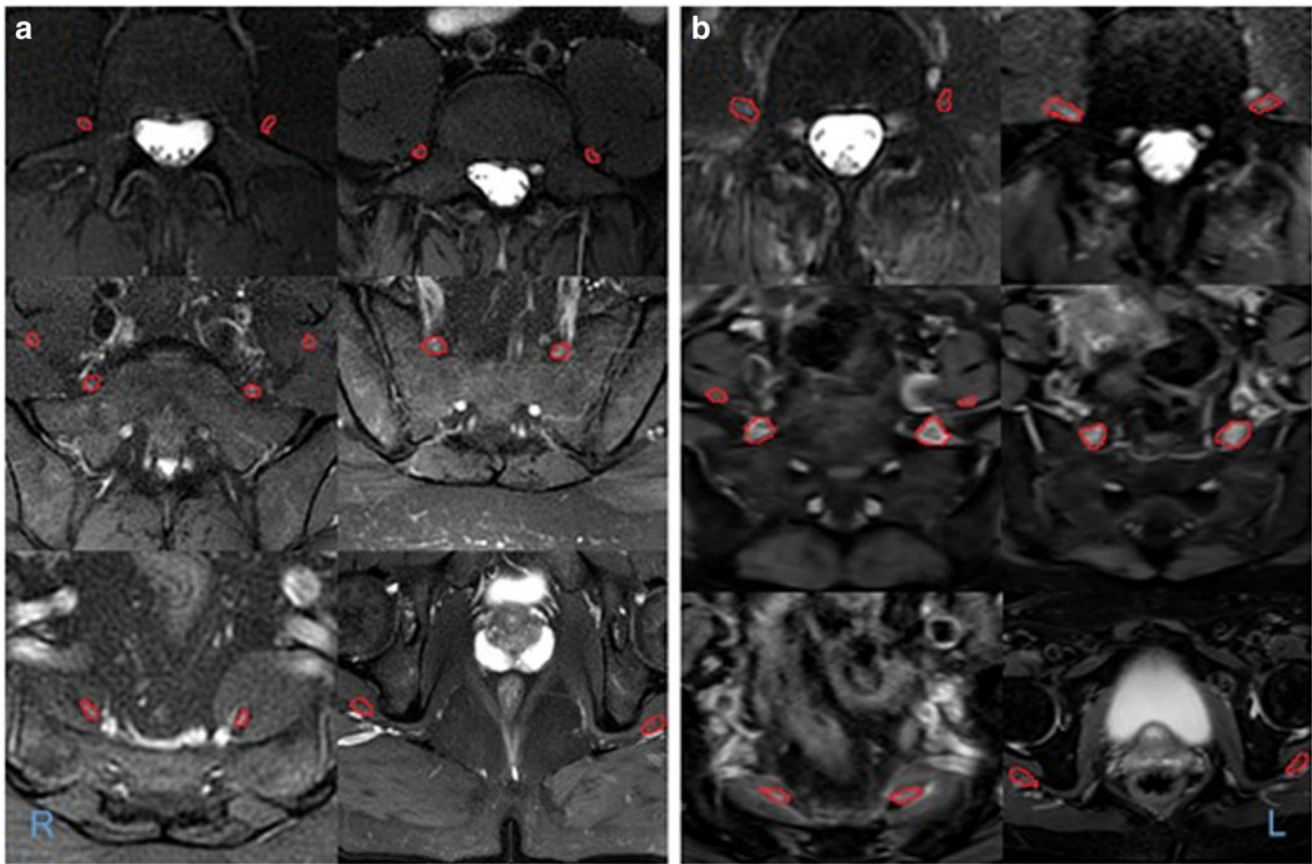


Fig. 1 Measurement (free hand best fit region of interest) of nerve roots and their peripheral branches. **a** Shown are the bilateral L3, L4, L5 and femoral, S1, S2, and sciatic nerves of a control patient carefully outlined

for measurement (left to right, nerves in red). **b** Shown are the bilateral L3, L4, and L5 and the femoral, S1, S2, and sciatic nerves of a DA carefully outlined for measurement (left to right, nerves in red)

coefficient (ICC) was then performed on measurements taken by reader 1 for intra-rater analysis. A linear model was performed to assess the nerve location and case/control effect on the nerve CSA. Both main effects and their interaction term were included. Within-patient correlation was adjusted by a random patient effect. Nerve CSA was log transformed using the natural log to correct for right skewness. The proximal and distal sciatic nerves were excluded (252 nerves) in the final analyses as both readers concluded that CSAs varied greatly depending on axial slice, and were not adequately cylindrical for correction by the model in Fig. 2. Eight nerves of the remaining 756 were further excluded in the final analysis based on missing data. Statistical analyses were performed using SAS 9.4 (SAS Institute, Inc.).

Results

Subjects

The basic demographics and clinical findings of the cases are outlined in Table 2 and Table 3, respectively. There were 14 females and 9 males ($p = 0.405$), all with type II DM. The

average patient age was 60.22 ± 14.63 ($p = 0.763$). The average patient BMI was 27.47 ± 5.16 ($p = 0.180$). DA had been diagnosed with diabetes for an average of 13.00 ± 9.18 years (5 with missing data). The average HbA1c closest to the time of lumbosacral plexus MRN was 7.70 ± 1.95 (1 patient with missing data). The average peak HbA1c was 9.34 ± 2.92 (1 patient with missing data). Seventeen DA (73.91%) presented with pain symptoms, 15 (65.22%) with motor symptoms, and 11 (47.83%) with sensory symptoms. Basic demographics of the controls are outlined in Table 2. The control sample consisted of 20 males and 20 females. The average patient age was 61.25 ± 12.00 years and the average patient BMI was 25.82 ± 4.33 . There was no significant difference between cases and controls with respect to sex, age, or BMI ($p = 0.405$, $p = 0.763$, and $p = 0.180$ respectively).

Ancillary tests

Fifteen DA (65.22%) had at least 1 prior, non-contributory MRI lumbar spine. Three DA (13.04%) had at least 1 prior, non-contributory MRI pelvis. Three DA (13.04%) had at least 1 prior, non-contributory MRI Knee.

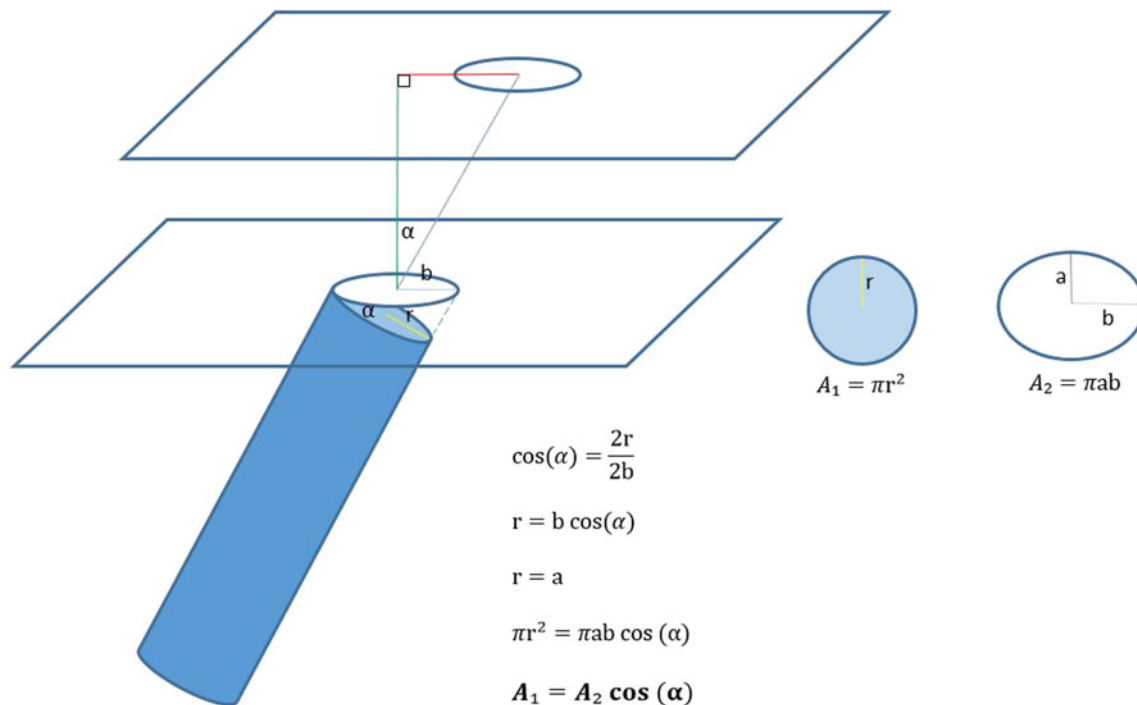


Fig. 2 Nerve trajectory correction factor. Shown is a nerve passing through two axial planes with an offset of angle α from the perpendicular. Angle α was calculated by taking the arc tangent of the ratio of the distance between centroids (red line) and the distance between

axial slices (green line). The true cross-sectional area of a nerve passing through a plane with an offset of α may be estimated by multiplying the measured ellipsoid area by cosine (α) as shown in the figure

Electrophysiology was conducted in 12 of 23 DA. Of those studies, 11 of 12 included all necessary (complete) NCS/EMG information for review. In 8/11 cases (72.72%), diabetic amyotrophy was included in the differential diagnosis of the impression by the fellowship-trained neuromuscular neurologist. In 5 of those 8 cases, diabetic amyotrophy was suggested as the most likely diagnosis.

Table 2 Demographics of cases and controls

	Cases		Controls	
	Count	Percentage of sample	Count	Percentage of sample
Sex				
Male	9	39.13	20	50.00
Female	14	60.87	20	50.00
Total	23	100.00	40	100.00
	Mean	Standard deviation	Mean	Standard deviation
Age				
Male	60.11	14.44	60.35	14.05
Female	60.29	15.30	62.15	9.83
Total	60.22	14.63	61.25	12.00
BMI (kg/m ²)				
Male	27.59	4.61	26.73	3.08
Female	27.39	5.65	24.92	5.22
Total	27.47	5.16	25.82	4.33

MRN findings

21/23 DA (91.30%) had abnormal nerve findings (thickening and/or hyperintensity) in the lumbosacral plexus nerve roots, and 16/23 (69.57%), 21/23 (91.30%), and 9/23 (39.13%) had lesions in either of the bilateral sciatic, femoral nerves, and the obturator nerves, respectively (Fig. 3). The signal alterations were not quantified as the scans were performed on different scanner strengths.

Fewer DA exhibited regional muscle denervation lesions as edema-like signal, fatty infiltration, and/or atrophy findings (Fig. 4).

In the majority of cases, MRN findings reflected the clinical symptoms of patients. MRN findings were concordant with the presence or absence of symptoms on either side of the body 82.61% (38/46) of the time. MRN findings were present without the presence of symptoms 17.39% (8/46) of the time. There were no cases where symptoms were reported without MRN findings present. Statistical analyses showed a strong relationship between sidedness of MRN findings and patient symptoms ($\chi^2(1) = 14.240, p < 0.001$; Φ coefficient = 0.556, $p < 0.001$).

With respect to the moderate to severe degenerative disc and joint disease, which could have been associated or mimicked radiculopathy/DA symptoms, 3/23 DA (13.04%) had findings in the L1 to L2 level, and 8/23 (34.78%), 10/23 (43.48%), 15/23 (65.22%), 13/23 (56.52%), and 3/23 (13.04%) in the L2 to L3 level, L3 to L4 level, L4 to L5 level, L5 to S1 level, and sacroiliac joints respectively.

Table 3 Clinical characteristics of diabetic amyotrophy (DA) patients

	Mean	Standard deviation
History of diabetes (years)	13.00	9.18
HbA1C closest time of MRN	7.70	1.95
Highest documented HbA1C	9.34	2.92
	Count	Percentage of sample
Patients with prior MRI		
MRI lumbar spine	15	65.22
MRI pelvis	3	13.04
MRI knee	3	13.04
Presenting symptom		
Pain	17	73.91
Motor	15	65.22
Sensory	11	47.83
Electrophysiological study outcome		
DA listed in the differential diagnosis	8 (5 ^a)	72.73
DA not listed in the differential diagnosis	3	27.27
Nerve lesions		
Lumbosacral plexus	21	91.30
Sciatic nerves	16	69.57
Femoral nerves	21	91.30
Obturator nerves	9	39.13
Muscle abnormalities		
Psoas major	7	30.43
Piriformis	11	47.83
Gluteal	15	65.22
Hamstrings	3	13.04
Proximal quadriceps	6	26.09
Adductors	11	47.83
Iliacus	1	4.35
Quadratus femoris	1	4.35
Para-spinal	7	30.43
Disc and joint degenerative changes		
L1 to L2	3	13.04
L2 to L3	8	34.78
L3 to L4	10	43.48
L4 to L5	15	65.22
L5 to S1	13	56.52
Sacroiliac joint	3	13.04

MRN magnetic resonance neurography

^a The number of times DA was listed as the most likely diagnosis within the given differential

Quantitative nerve findings

The linear model did not show evidence of a significant interaction effect between group (DA or control group) and nerve location ($p = 0.9792$). Both main effects, however, were significant. Nerve locations were significantly different in size

($p < 0.001$). DA nerves were significantly larger than control nerves ($p < 0.001$). Nerve location was controlled for because CSA varies between nerve roots. Three DA cases had 4/12 (33.33%), 2/12 (16.67%), and 2/12 (16.67%) respective nerves missing from the final data set of 756 nerves. The estimated marginal mean nerve CSAs were 45% greater in cases than controls (95% CI, (30%, 49%)).

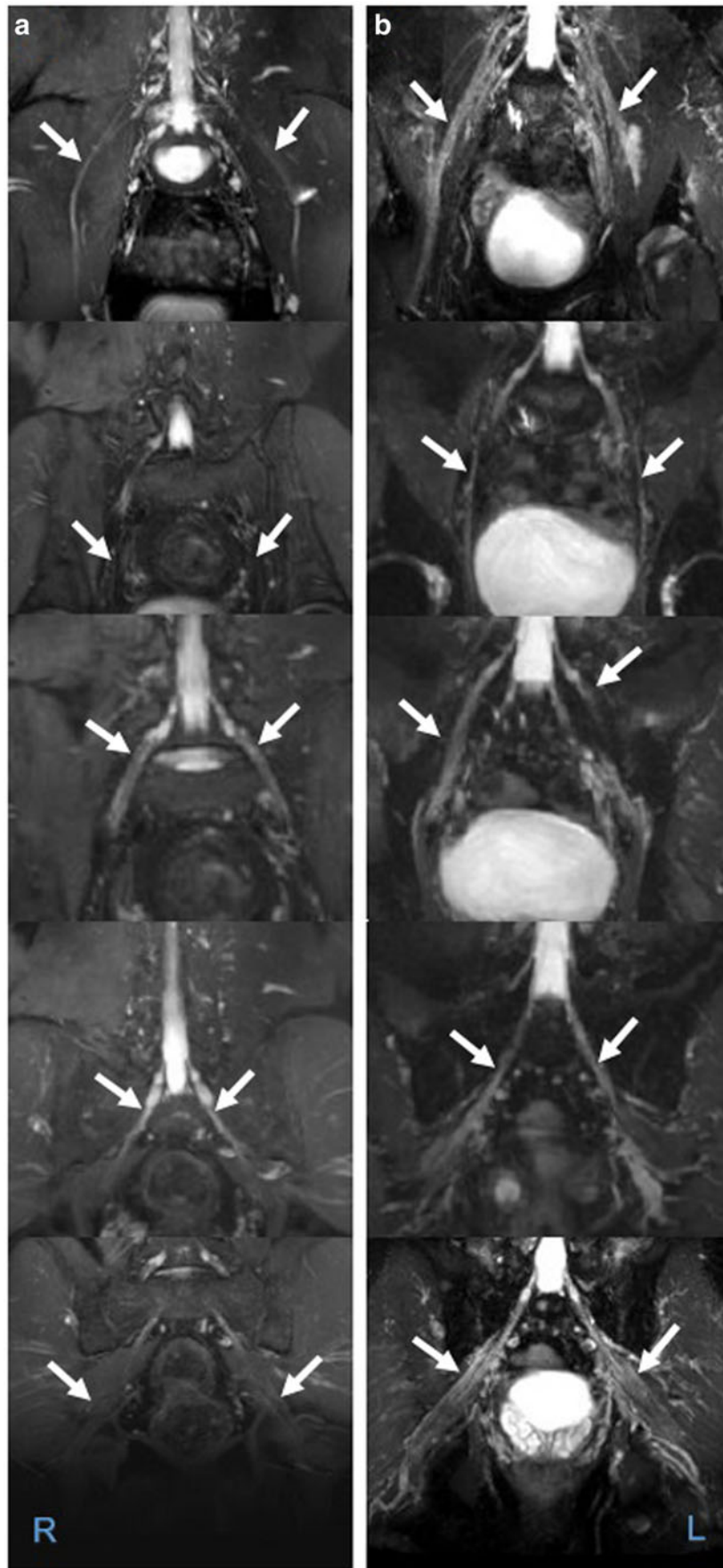
The ICC between the readers was 0.547 upon exclusion of the proximal and distal sciatics (95% CI, 0.456 to 0.626). The ICC between reader R1’s initial and second measurements was 0.90 (95% CI, 0.89–0.92). The ICC between the readers was 0.378 with inclusion of the proximal and distal sciatics (95% CI, 0.267 to 0.477).

Discussion

In this systematic analysis, we found that the lumbosacral nerve roots and femoral nerves of individuals with DA are significantly larger in CSA than those of controls. Observed differences in DA lumbosacral nerve CSAs are in agreement with previous studies of diabetic nerve CSA measured on ultrasound and focused MRI [15, 18, 20, 21]. Changes to the gross nerve morphology in diabetic neuropathy is caused by multiple histologic alterations, such as hypertrophy and hyperplasia of endothelial cells, pericyte and endoneurial cell damage, and thickened perineural basement membranes [22, 23]. The exact mechanism by which these changes occur is controversial, but may be due to accumulation of glycation and advanced glycation end products, the polyol pathway, oxidative stress, PKC activity, pro-inflammatory processes, or any combination of these [23, 24]. Kawamura et al found that ICAM1, TNF alpha, and NFκB were seen predominantly in DA nerve biopsies versus controls [25]. Furthermore, several retrospective studies have demonstrated improvement of DA symptoms with anti-inflammatory or immunosuppressive therapies in agreement with an inflammatory mediated picture [26–28]. Pathological changes related to inflammation are consistent with the hyperintensity and/or nerve thickening seen on MRN in DA cases [7, 29].

Several nerves and muscles exhibited qualitative signal and caliber alterations as discussed in the results. This has been previously described in the literature [15, 29]. However, we

Fig. 3 3-D reconstructed thick slab maximum intensity projections of the LS plexus and nerves: DA and controls. **a** Shown are the femoral nerves, obturator nerves, L5 nerves, S1 nerves, and sciatic nerves of a control patient (top to bottom, indicated by arrows). **b** Shown are the femoral nerves, obturator nerves, L5 nerves, S1 nerves, and sciatic nerves (top to bottom, indicated by arrows) of a DA who was admitted for right lower extremity weakness that progressed to involve the left lower extremity. Bilateral L4 to S2 nerves, sciatic nerves, femoral nerves, and obturator nerves are increased in size and signal bilaterally on magnetic resonance neurography



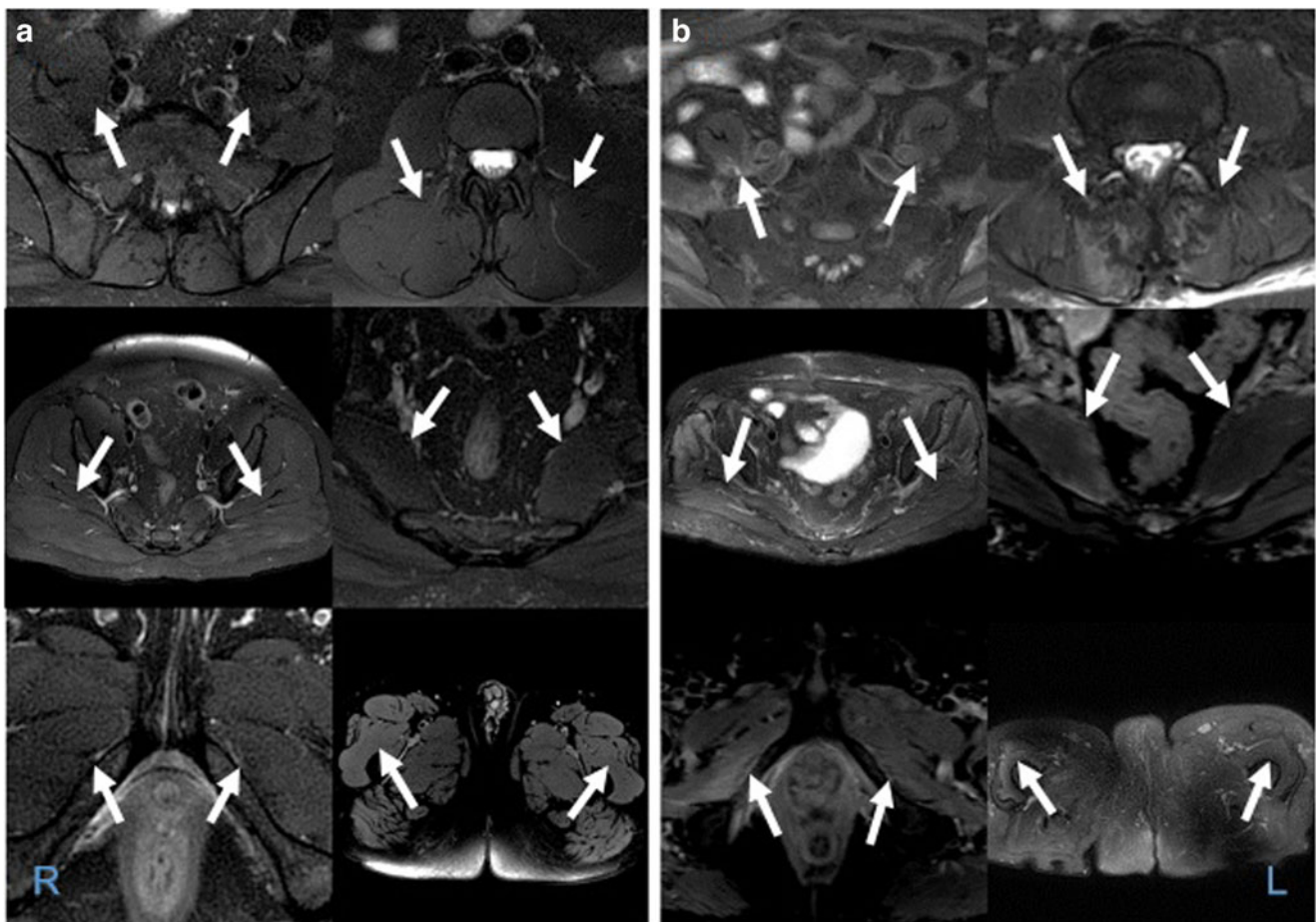


Fig. 4 3-D reconstructed nerves of DA and controls. **a** Shown are the psoas, para-spinal, gluteal, piriformis, adductor, and proximal quadriceps muscles of a control patient (left to right, indicated by arrows). **b** Shown are the psoas, para-spinal, gluteal, piriformis, adductors, and proximal quadriceps muscles of DA (left to right, indicated by arrows). There is a denervation edema-like signal in the right psoas muscle. There is a patchy

edema-like signal in the bilateral para-spinal muscles. There is a denervation edema-like signal and atrophy of the bilateral gluteal muscles. There is an edema-like signal in the right adductors. There is mild atrophy of the right piriformis with mild edema-like signal. There is a patchy edema-like signal and atrophy of the right quadriceps muscle

did not quantitatively explore intensities of the nerves as the MRN exams had been formally read as a standard of care, and the cases and controls were selected from different magnet strengths that would confound observed signal alterations.

In this study, the electrophysiology studies suggested DA as most likely in 5/11 cases, and included the diagnosis of DA in 8/11 cases. It has been reported that electrophysiological testing may be confirmatory in later stages of DA but is often non-diagnostic early on [30, 31]. It might be the case in our series that more complicated or clinically confusing cases were sent for MRN examination. In all cases, MRN detected multifocal nerve abnormalities and regional muscle denervation changes. In addition, MRN was able to exclude the confounding diagnoses of radiculopathy, entrapment, and mass lesion, since in all cases, multiple nerves were diffusely abnormal and muscle lesions were multifocal. In a patient with DM presenting with severe neuropathic pain followed by progressive weakness, the findings of neuromuscular lesions on electrophysiology and MRN can aid in establishing the diagnosis of DA.

Similarly, a majority of DA cases in this study had also received prior conventional MR imaging (lumbar spine, pelvis, knee) that was non-contributory. Average HbA1C levels of DA cases were mildly elevated in our sample (7.70 ± 1.95), similar to the previous reports [5, 31]. Furthermore, HbA1C levels did not correlate with nerve CSAs, further suggesting that development of DA may not be proportional to the glucose control. Presenting symptoms in our case series were predominantly pain and weakness as is generally the case in DA [5].

There are several limitations to this study. The study is retrospective and sample size is small, limiting generalizability. Another limitation involves the use of ROI measurements from the axial slices. The paths taken by nerves of interest are not perpendicular to the axial plane in all cases. Although a correction coefficient was used to mitigate overestimation of nerve CSA, the derivation of this correction factor was based upon a perfectly cylindrical object traveling in a straight line between adjacent axial slices. Deviation from this model will introduce error, although it should be less than without

correction. Strengths of this study include the use of 3.0-T imaging in the majority of cases. 3.0-T scanners allow greater anatomic detail than 1.5-T scanners [32, 33]. To date, this is the only systematic study of our knowledge that has examined the anatomical characteristics of the lumbosacral plexus in DA using MRN. We did not use DM patients with clinical findings or symptoms of DA. Future directions include prospective assessment of signal intensity alterations, comparison with DM controls, and diffusion characteristics of nerves on MRN performed on a single scanner in a larger cohort of patients and controls.

To summarize, DA-related multifocal neuromuscular lesions can be qualitatively and quantitatively detected on MRN, and as a non-invasive diagnostic tool, it can be employed for the evaluation of patients with diabetic radiculoplexopathy.

Funding The authors state that this work has not received any funding.

Compliance with ethical standards

Guarantor The scientific guarantor of this publication is Avneesh Chhabra.

Conflict of interest Avneesh Chhabra declares relationships with the following companies: consultant for ICON Medical and receives royalties from Jaypee and Wolters. All other authors have no relationships to declare.

Statistics and biometry Yin Xi, PhD (University of Texas Southwestern Medical Center), has significant statistical expertise.

Informed consent Written informed consent was waived by the Institutional Review Board.

Ethical approval Institutional Review Board approval was obtained.

Methodology

- retrospective
- cross-sectional study
- performed at one institution

References

1. Centers for Disease Control and Prevention (2017) National Diabetes Statistics Report, 2017. Available via <https://www.cdc.gov/diabetes/pdfs/data/statistics/national-diabetes-statistics-report.pdf>. Accessed 4/12/2018
2. Tancredi M, Rosengren A, Svensson AM et al (2015) Excess mortality among persons with type 2 diabetes. *N Engl J Med* 373:1720–1732
3. American Diabetes Association (2013) Economic costs of diabetes in the U.S. in 2012. *Diabetes Care* 36:1033–1046
4. Sytze Van Dam P, Cotter MA, Bravenboer B, Cameron NE (2013) Pathogenesis of diabetic neuropathy: focus on neurovascular mechanisms. *Eur J Pharmacol* 719:180–186
5. Dyck PJ, Norell JE, Dyck PJ (1999) Microvasculitis and ischemia in diabetic lumbosacral radiculoplexus neuropathy. *Neurology* 53: 2113–2121
6. Stoll G, Bendszus M, Perez J, Pham M (2009) Magnetic resonance imaging of the peripheral nervous system. *J Neuro* 256:1043
7. Thakkar RS, Del Grande F, Thawait GK, Andreisek G, Carrino JA, Chhabra A (2012) Spectrum of high-resolution MRI findings in diabetic neuropathy. *AJR Am J Roentgenol* 199:407–412
8. Delaney H, Bencardino J, Rosenberg ZS (2014) Magnetic resonance neurography of the pelvis and lumbosacral plexus. *Neuroimaging Clin N Am* 24:127–150
9. London ZN (2016) Safety and pain in electrodiagnostic studies. *Muscle Nerve* 55:149–159
10. Winkel J, Jørgensen K (1991) Significance of skin temperature changes in surface electromyography. *Eur J Appl Physiol Occup Physiol* 63:345–348
11. Brody LR, Pollock MT, Roy SH, De Luca CJ, Celli B (1991) pH-induced effects on median frequency and conduction velocity of the myoelectric signal. *J Appl Physiol* (1985) 71:1878–1885
12. Kuiken TA, Lowery MM, Stoykov NS (2003) The effect of subcutaneous fat on myoelectric signal amplitude and cross-talk. *Prosthet Orthot Int* 27:48–54
13. Chhabra A, Andreisek G, Soldatos T et al (2011) MR neurography: past, present, and future. *AJR Am J Roentgenol* 197:583–591
14. Filler AG, Maravilla KR, Tsuruda JS (2004) MR neurography and muscle MR imaging for image diagnosis of disorders affecting the peripheral nerves and musculature. *Neuro* 22:643–682
15. Pham M, Oikonomou D, Bäumer P et al (2011) Proximal neuropathic lesions in distal symmetric diabetic polyneuropathy: findings of high-resolution magnetic resonance neurography. *Diabetes Care* 34:721–723
16. Pham M, Oikonomou D, Hornung B et al (2015) Magnetic resonance neurography detects diabetic neuropathy early and with proximal predominance. *Ann Neurol* 78:939–948
17. Jende JME, Groener JB, Oikonomou D et al (2018) Diabetic neuropathy differs between type 1 and type 2 diabetes: insights from magnetic resonance neurography. *Ann Neurol* 83:588–598
18. Vaeggemose M, Pham M, Ringgaard S et al (2017) Magnetic resonance neurography visualizes abnormalities in sciatic and tibial nerves in patients with type 1 diabetes and neuropathy. *Diabetes* 66:1779–1788
19. Robbins NM, Shah V, Benedetti N, Talbott JF, Chin CT, Douglas VC (2016) Magnetic resonance neurography in the diagnosis of neuropathies of the lumbosacral plexus: a pictorial review. *Clin Imaging* 40:1118–1130
20. Lee D, Dauphinée DM (2005) Morphological and functional changes in the diabetic peripheral nerve: using diagnostic ultrasound and neurosensory testing to select candidates for nerve decompression. *J Am Podiatr Med Assoc* 95:433–437
21. Kang S, Kim SH, Yang SN, Yoon JS (2016) Sonographic features of peripheral nerves at multiple sites in patients with diabetic polyneuropathy. *J Diabetes Complications* 30:518–523
22. Hill RE, Williams PE (2004) Perineurial cell basement membrane thickening and myelinated nerve fibre loss in diabetic and nondiabetic peripheral nerve. *J Neurol Sci* 217:157–163
23. Yagihashi S, Mizukami H, Sugimoto K (2011) Mechanism of diabetic neuropathy: where are we now and where to go? *J Diabetes Investig* 2:18–32
24. Tang WH, Martin KA, Hwa J (2012) Aldose reductase, oxidative stress, and diabetic mellitus. *Front Pharmacol* 3:87
25. Kawamura N, Dyck PJ, Schmeichel AM, Engelstad JK, Low PA, Dyck PJ (2008) Inflammatory mediators in diabetic and non-diabetic lumbosacral radiculoplexus neuropathy. *Acta Neuropathol* 115:231–239
26. Pascoe MK, Low PA, Windebank AJ, Litchy WJ (1997) Subacute diabetic proximal neuropathy. *Mayo Clin Proc* 72:1123–1132

27. Krendel DA, Costigan DA, Hopkins LC (1995) Successful treatment of neuropathies in patients with diabetes mellitus. *Arch Neurol* 52:1053–1061
28. Tamburin S, Magrinelli F, Favaro F, Briani C, Zanette G (2014) Long-term response of neuropathic pain to intravenous immunoglobulin in relapsing diabetic lumbosacral radiculoplexus neuropathy. A case report. *Pain Pract* 14:E85–E90
29. Soldatos T, Andreisek G, Thawait GK et al (2013) High-resolution 3-T MR neurography of the lumbosacral plexus. *Radiographics* 33: 967–987
30. Dyck PJ, Norell JE, Dyck PJ (2001) Non-diabetic lumbosacral radiculoplexus neuropathy: natural history, outcome and comparison with the diabetic variety. *Brain* 124:1197–1207
31. Dyck PJ, Windebank AJ (2002) Diabetic and nondiabetic lumbosacral radiculoplexus neuropathies: new insights into pathophysiology and treatment. *Muscle Nerve* 25:477–491
32. Schmid-Schwap M, Drahanowsky W, Bristela M, Kundi M, Piehslinger E, Robinson S (2009) Diagnosis of temporomandibular dysfunction syndrome—image quality at 1.5 and 3.0 Tesla magnetic resonance imaging. *Eur Radiol* 19:1239–1245
33. Stehling C, Bachmann R, Langer M, Nassenstein I, Heindel W, Vieth V (2009) High-resolution magnetic resonance imaging of triangular fibrocartilage complex lesions in acute wrist trauma: image quality at different field strengths. *J Comput Assist Tomogr* 33: 579–583

Publisher's note Springer Nature remains neutral with regard to jurisdictional claims in published maps and institutional affiliations.